Available online at www.sciencedirect.com
ScienceDirect
Thermochimica Acta 450 (2006) 105–109
thermochimica acta
www.elsevier.com/locate/tca

Heat capacity, enthalpy and entropy of strontium bismuth niobate and strontium bismuth tantalate

J. Leitner [a,*], M. Hampl [a], K. Růžička [b], D. Sedmidubský [c], P. Svoboda [d], J. Vejpravová [d]

[a] *Department of Solid State Engineering, Institute of Chemical Technology, Technická 5, 166 28 Prague 6, Czech Republic*
[b] *Department of Physical Chemistry, Institute of Chemical Technology, Technická 5, 166 28 Prague 6, Czech Republic*
[c] *Department of Inorganic Chemistry, Institute of Chemical Technology, Technická 5, 166 28 Prague 6, Czech Republic*
[d] *Department of Electronic Structures, Faculty of Mathematics and Physics, Charles University, Ke Karlovu 5, 120 00 Prague 2, Czech Republic*

Available online 19 September 2006

Abstract

The heat capacities and enthalpy increments of strontium bismuth niobate $SrBi_2Nb_2O_9$ (SBN) and strontium bismuth tantalate $SrBi_2Ta_2O_9$ (SBT) were measured by the relaxation method (2–150 K), Calvet-type heat-conduction calorimetry (305–570 K) and drop calorimetry (773–1373 K). The temperature dependences of non-transition heat capacities in the form $C_{pm} = 324.47 + 0.06371T - 5.0755 \times 10^6/T^2$ J K^{-1} mol^{-1} (298–1400 K) and $C_{pm} = 320.22 + 0.06451T - 4.7001 \times 10^6/T^2$ J K^{-1} mol^{-1} (298–1400 K) were derived for SBN and SBT, respectively, by the least-squares method from the experimental data. Furthermore, the standard molar entropies at 298.15 K S°_m(SBN) = 327.15 ± 0.80 and S°_m(SBT) = 339.23 ± 0.72 J K^{-1} mol^{-1} were evaluated from the low-temperature heat capacity measurements.

Keywords: $SrBi_2Nb_2O_9$; $SrBi_2Ta_2O_9$; Strontium bismuth niobate; Strontium bismuth tantalate; Heat capacity; Enthalpy increment; Entropy

1. Introduction

Ceramic materials with ferroelectric properties have found many applications in electronics and optics. In the semiconductor industry, much attention is paid to materials used in non-volatile ferroelectric random access memories (FeRAM). At the present time, PZT ($PbZr_{1-x}Ti_xO_3$) ceramics are generally used for FeRAM fabrication. Bismuth layered perovskites $SrBi_2Ta_2O_9$ (SBT) and $SrBi_2Nb_2O_9$ (SBN) are now being extensively studied because of their lower fatigue, better compatibility with CMOS (complementary metal-oxide-semiconductor) technology and lead-free composition [1–3]. Both ferroelectric compounds are orthorhombic (space group $A2_1am$) at room temperature and transform to tetragonal paraelectric phases (space group $I4/mmm$) above the Curie temperature T_C. Various values of the ferroelectric transition temperature T_C derived from dielectric constant measurements with sintered powder samples are given in literature: T_C = 543–608 K for SBT [4–10] and 687–723 K for SBN [4,5,8,11,12].

SBT, SBN, and their solid solutions have been prepared as powder materials as well as thin films by a number of methods. Metalorganic chemical vapor deposition (MOCVD) has been investigated as the most practical preparation method to realize a high-density FeRAM because of the good step coverage and the uniform composition and film thickness over a large area. For better understanding of MOCVD processes, thermodynamic calculations of equilibrium compositions of relevant systems are often performed. For such a calculation, thermodynamic data for all considered substances are necessary.

Morimoto et al. [5] measured the heat capacities of SBT and SBN in the temperature range 500–770 K by the thermal radiation calorimetry. Their measurements were performed with powder samples of approximately 5 g. While the temperature dependence of the heat capacity of SBT does not show any anomaly in this temperature region, a distinct peak with maximum at 678 K was observed for SBN. Temperature dependence of the heat capacity of SBT in the form of polycrystalline sample, single crystal as well as thin film were also determined by Onodera et al. [13–15]. The measurements were performed in the temperature range 80–800 K. A slight hump in C_p was observed around 610 K for a polycrystalline sample, while a rather clear anomaly was detected at 613 K for the single crystal

* Corresponding author. Fax: +420 220 444 330.
E-mail address: jindrich.leitner@vscht.cz (J. Leitner).

0040-6031/$ – see front matter © 2006 Elsevier B.V. All rights reserved.
doi:10.1016/j.tca.2006.09.006

sample. Yin et al. [16] DSC study of phase transitions of SBT detected two anomalies around 601 and 838 K, the first is a ferroelectric transition while the second one was supposed to be a structural transition. This observation is in agreement with the results obtained by Macquart et al. [7] who found such a transition from orthorhombic to tetragonal structure above 773 K. Enthalpy changes of these transitions are 293 and 212 J mol^{-1}, respectively [16].

As part of a systematic study of thermodynamic properties of mixed oxides in the system Bi_2O_3–SrO–CaO–Ta_2O_5–Nb_2O_5 [17,18], heat capacities and enthalpy increments of SBN and SBT were measured with various calorimetric techniques. Moreover, values of the standard molar entropies at 298.15 K have been evaluated for both oxides by integration of C_{pm}/T functions from 0 to 298.15 K.

2. Experimental

Powder samples of SBN and SBT were prepared by conventional solid-state reaction from pure carbonate and binary oxides. The starting materials $SrCO_3$ (99.9%, Aldrich), Bi_2O_3 (99.9%, Aldrich), and Nb_2O_5 (99.85%, Alfa) or Ta_2O_5 (99.85%, Alfa) in stoichiometric amounts were mixed and ground in an agate mortar. The $SrCO_3$–Bi_2O_3–Nb_2O_5 mixture was treated in Pt crucible at 1273 K for 24 h in air, and, after homogenization, at 1473 K for 24 h in air while the $SrCO_3$–Bi_2O_3–Ta_2O_5 mixture was heated at 1073 K for 24 h, and, after homogenization, at 1273 K for 120 h, both in air. Powder X-ray diffraction data were collected on a PANalytical X'Pert PRO diffractometer using Cu Kα radiation. The scan rate of 4° 2θ/min in the range 5–75° 2θ was used for XRD data collection. The detection limit for minority phases was 2 wt.%.

Both oxides can show some nonstoichiometry and therefore the exact stoichiometry of our samples was determined. X-ray fluorescence spectroscopy (ARL 9400, Thermo Electron Corporation) was used for chemical analysis. The effective masses of samples with the 0.7 mm height were 1040 mg (SBN) and 1106 mg (SBT). The standardless method UniQuant 4 [19] was used for quantitative determination.

The PPMS equipment (Quantum Design) was used for heat capacity measurements in the low-temperature region. The samples for the PPMS apparatus were compressed powder plates of about 15 mg. Density of pressed sample was 75.5% of theoretical in the case of SBN and 63.3% for SBT. The sample was mounted to the calorimeter platform with Apiezon N grease. A sample holder with the Apiezon only was measured in the temperature range 2–300 K to obtained background data, then the sample plate was attached to the calorimeter platform with Apiezon and the measurement was repeated in the same temperature range with the same temperature steps. The sample specific heat was then obtained as the difference of the two data sets. The specific heat of Apiezon is not negligible in comparison with the specific heat of the sample (∼8% at the room temperature) and exhibits a sol–gel transition below the room temperature [20].

The heat capacity measurements in the PPMS were performed by the relaxation method [21] with fully automatic procedure under high vacuum (pressure ∼10^{-2} Pa) to avoid heat loss through the exchange gas. The manufacturer's claim of better then 2% accuracy [22] was confirmed by measurements on a copper sample (99.999% purity). The accuracy of the measurement depends strongly on the thermal coupling between the sample and the calorimeter platform. Due to unavoidable porosity of the sample plate, this coupling becomes rapidly worse at temperatures above 200 K as the Apiezon diffuses into the porous sample. Thus only the data up to 150 K were taken as reliable and used for calculations.

The Setaram C-80 calorimeter was used for heat capacity determinations from 305 to 570 K. The measurements were carried out in the incremental temperature scanning mode with a number of 5–10 K steps (heating rate 0.2 K min^{-1}) followed by isothermal delays of 9000 s. Three runs were performed: with empty crucible (blank), with the reference material (synthetic sapphire, NIST Standard reference material No. 720) and with the sample (SBN or SBT). The typical mass of samples was 13–16 g. The accuracy of the heat capacity measurements is estimated to be better than ±2%.

Enthalpy increment determinations were carried out by the drop method in a Setaram Multi HTC 96 high-temperature calorimeter. All measurements were performed in air by alternating dropping of the reference material (small pieces of synthetic sapphire, NIST Standard reference material No. 720) and of the sample (SBN or SBT pellets, 5 mm in diameter, thickness 1.5–2.5 mm) being initially held at room temperature (T_0) through a lock into the working cell of the preheated calorimeter. Measurements were performed at 773–1373 K on samples with typical masses 230–380 mg. Delays between subsequent drops were 40–50 min. To check the accuracy of the measurement, the heat content of platinum was measured first and compared with published values [23–25]. Estimated overall accuracy of the drop measurements is ±3%.

3. Results and discussion

The XRD analysis revealed that the prepared samples consist of single phase SBN or SBT. Both were present in orthorhombic structure (space group $A2_1am$). The lattice parameters of the samples were evaluated by Rietveld refinement using published atomic positions [26]: $a = 0.551599 \pm 0.00052$ nm, $b = 0.550868 \pm 0.00054$ nm and $c = 2.51020 \pm 0.00193$ nm for SBN and $a = 0.552244 \pm 0.00039$ nm, $b = 0.552662 \pm 0.00039$ nm and $c = 2.50124 \pm 0.00101$ nm for SBT. These are in good agreement with the values published recently [7,27–29].

Based on the X-ray fluorescence spectroscopy analysis, the compositions of our samples are: (11.89 ± 0.16) wt.% SrO, (55.08 ± 0.25) wt.% Bi_2O_3 and (33.01 ± 0.24) wt.% Nb_2O_5 for SBN and (10.16 ± 0.15) wt.% SrO, (45.08 ± 0.25) wt.% Bi_2O_3 and (44.66 ± 0.25) wt.% Ta_2O_5 for SBT. This corresponds to $Sr_{0.92}Bi_{1.91}Nb_{2.00}O_{8.33}$ and $Sr_{0.97}Bi_{1.91}Ta_{2.00}O_{8.35}$. The oxygen stoichiometry was not determined but calculated with valence of metal ions Sr^{2+}, Bi^{3+} and Nb^{5+}. Calcium oxide was detected as the most abundant impurity: 0.03 wt.% CaO in SBN and 0.01 wt.% CaO in SBT. Bismuth is in a slight deficit in both

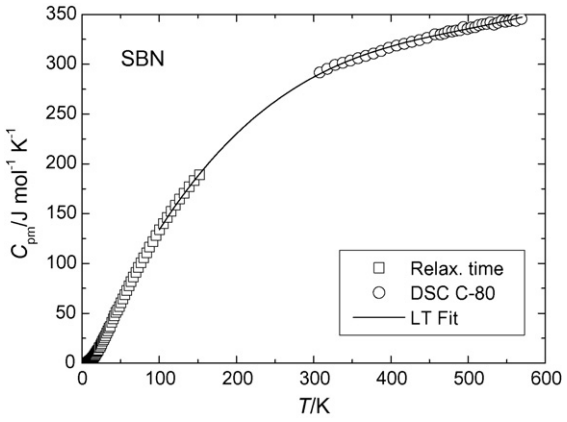

Fig. 1. Temperature dependence of the heat capacity of SBN (LT Fit—low-temperature fit calculated according to Eq. (1) with parameters mentioned in Table 1).

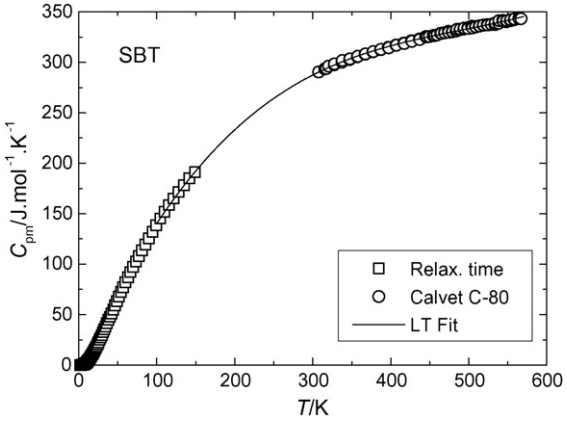

Fig. 2. Temperature dependence of the heat capacity of SBT (LT Fit—low-temperature fit calculated according to Eq. (1) with parameters mentioned in Table 1).

cases, explained by significant volatility of bismuth oxide during the synthesis at high temperatures. The same effect was observed by Zurbuchen et al. on SBN and SBT films [30].

The measured C_{pm} data (95 and 94 points from relaxation time and 38 and 76 points from heat-conduction calorimetry for SBN and SBT, respectively) are summarized in supplementary Tables 1 and 2 and plotted in Figs. 1 and 2. The enthalpy increment data (28 and 19 points for SBN and SBT, respectively) are listed in supplementary Tables 3 and 4.

The raw data were analyzed in two separate steps by the least-squares method with different weights for individual points. Data at 100–150 K and data at 305–570 K were fitted using an empirical polynomial equation:

$$C_{pm} = A + BT + CT^2 + DT^3 \quad (1)$$

The parameters of Eq. (1) are given in Table 1 together with their standard deviations (2σ). C_{pm}(SBN, 298.15 K) = 286.37 J K^{-1} mol^{-1} and C_{pm}(SBT, 298.15 K) = 286.58 J K^{-1} mol^{-1} were calculated from Eq. (1) and these values subsequently used as constraints for processing high-temperature data.

For the assessment of C_{pm} functions above room temperature, the heat capacity data from heat-conduction calorimetry and the enthalpy increment data from drop calorimetry were treated simultaneously. Because our measurements were performed out of the ferroelectric transition region the derived equations hold for non-transition heat capacity only omitting C_{pm} anomalies in the vicinity of T_C which were observed by other authors [5,13–15]. We supposed that ferroelectric transitions of SBT and SBN above room temperature, accompanied by continuous structural transitions (orthorhombic → tetragonal) [7], are of the second-order without any step changes in enthalpy. Thus it is possible to use only one equation for the whole temperature interval. As the heat effect due to the ferroelectric transition is small [16] compared to the enthalpy increments and their deviations, no additional corrections were made. Different weights w_i were assigned to individual points calculated as $w_i = 1/\delta_i^2$, where δ_i is absolute deviation of the ith measurement estimated from overall accuracies of the measurements (2% for heat-conduction calorimetry and 3% for drop calorimetry). Both types of experimental data thus gain comparable significance during the regression analysis. The temperature dependence of the non-transition molar heat capacity of solid SBN and SBT can thus be expressed by (T = 298.15–1400 K):

$$C_{pm}(\text{SBN})\,(\text{J K}^{-1}\,\text{mol}^{-1}) = (324.47 \pm 7.48) + (0.06371 \pm 0.01172)T - \frac{(5.0755 \pm 0.3604) \times 10^6}{T^2} \quad (2)$$

$$C_{pm}(\text{SBT})\,(\text{J K}^{-1}\,\text{mol}^{-1}) = (320.22 \pm 5.29) + (0.06451 \pm 0.00859)T - \frac{(4.7001 \pm 0.2449) \times 10^6}{T^2} \quad (3)$$

The heat capacity as a function of temperature for SBN and SBT according to Eqs. (2) and (3) is shown in Fig. 3. While the heat capacities of both oxides are almost the same at 298 K,

Table 1
Parameters A, . . ., D of Eq. (1)

	SBN		SBT	
	Parameter	Standard deviation (2σ)	Parameter	Standard deviation (2σ)
A	−14.77	4.00	−4.80	2.524
B	1.793	0.051	1.754	0.0319
C	−0.0033	0.0002	−0.0033	0.0001
D	2.189×10^{-6}	1.666×10^{-7}	2.223×10^{-6}	1.029×10^{-7}

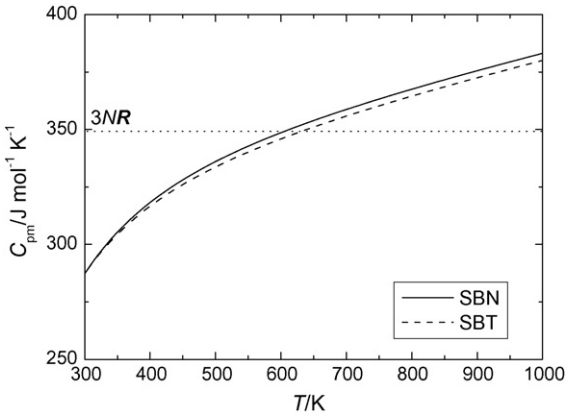

Fig. 3. High-temperature dependences of the heat capacity of SBN and SBT calculated according to Eqs. (2) and (3). Dotted line represents the Dulong–Petit limit.

there is a small constant difference of ∼3 J mol^{-1} K^{-1} in high-temperature limit, which is in accord with the slightly higher values of enthalpy increments for SBN in comparison with SBT. This can be a result of a more pronounced heat effect associated with the ferroelectric transition as reported by Morimoto et al. [5]. Indeed, a subtraction of this effect (∼2.5 kJ mol^{-1}) from our enthalpy increment data leads to a corresponding suppression of the resulting C_{pm} above the transition, such that the two curves become nearly identical.

A comparison with the published heat capacity data is difficult because these are presented only as plots. Values read from graphs [5] and those calculated from Eqs. (2) and (3) are: C_{pm}(SBN, 507.4 K) = 326.8 and 337.1 J K^{-1} mol^{-1}, C_{pm}(SBN, 744.6 K) = 360.2 and 362.8 J K^{-1} mol^{-1}, C_{pm}(SBT, 508.1 K) = 328.4 and 334.7 J K^{-1} mol^{-1} and C_{pm}(SBT, 745.1 K) = 379.1 and 358.8 J K^{-1} mol^{-1}, respectively.

The values of standard molar entropies of SBN and SBT at 298.15 K were derived from the low-temperature C_{pm} data by integrating the C_{pm}/T functions from 0 to 298.15 K. A numerical integration was used for the 0–150 K range using the trapezoid rule with the boundary conditions $S^{\circ}_{m}(0\,K) = 0$ and $C_{pm}/T = 0$ for $T = 0$ K. An analytical integration of Eq. (1) with the parameters listed in Table 1 was applied from 150 to 298.15 K. Standard deviations (2σ) were calculated using the error propagation law. These values as well as the standard entropies of formation from the constituent binary oxides, $\Delta S_{f,ox}$, are summarized in Table 2. The higher value of S°_{m}(298.15 K) obtained for SBT is apparently due to higher values of C_{pm}/T in the temperature range 25–150 K, whereas in low-temperature limit and for 150–300 K, both curves lie very close to each other. Regarding the chemical similarity of Nb and Ta this effect is presumably linked to higher atomic weight of Ta causing the excitation of the corresponding phonon modes at lower temperatures. The values of $\Delta S_{f,ox}$ for other mixed oxides in the system Bi_2O_3–SrO–Ta_2O_5–Nb_2O_5 are also listed in Table 2 for comparison.

Table 2
Standard molar entropies and standard entropies of formation of mixed oxides from the constituent binary ones

Oxide	S°_{m}(298.15 K) (J K^{-1} mol^{-1})	$\Delta S_{f,ox}$(298.15 K) (J K^{-1} mol^{-1})
Bi_2O_3	148.5 [31]	
SrO	53.58 [32]	
Nb_2O_5	137.30 [33]	
Ta_2O_5	143.09 [33]	
$SrBi_2Nb_2O_9$	327.15 ± 0.80[a]	−12.23
$SrBi_2Ta_2O_9$	339.23 ± 0.72[a]	−5.94
$SrBi_2O_4$		−12[b]
$Sr_2Bi_2O_5$		−24[b]
$Sr_3Bi_2O_6$		−7[b]
$BiNbO_4$	147.86[c]	4.96
$BiTaO_4$	149.11[c]	3.31
$Sr_2Nb_2O_7$	232.37[d]	−12.09
$Sr_2Ta_2O_7$	245.41[d]	−4.84
$Sr_2Nb_2O_7$		−39.93[e]
$Sr_2Nb_{10}O_{27}$		−350.69[e]
$Sr_5Nb_4O_{15}$		−51.01[e]

[a] This work.
[b] Thermodynamic assessment [34].
[c] Based on low-temperature calorimetric data [18].
[d] Based on low-temperature calorimetric data [35].
[e] Thermodynamic assessment [36].

Acknowledgements

This work was supported by the Ministry of Education of the Czech Republic (Research Projects No. MSM6046137302 and No. MSM6046137307). The work of PS and JV is a part of the research program MSM0021620834 financed by the Ministry of Education of the Czech Republic.

Appendix A. Supplementary data

Supplementary data associated with this article can be found, in the online version, at doi:10.1016/j.tca.2006.09.006.

References

[1] J.F. Scott, Topics in applied physics in: H. Ischiwara, M. Okuyama, Y. Arimoro (Eds.), Ferroelectric Random Access Memories, vol. 93, Springer, Berlin-Heideberg, 2004, pp. 3–16.
[2] Y. Arimoto, H. Ischiwara, MRS Bull. 29 (2004) 823.
[3] H. Kohlstedt, Y. Mustafa, A. Gerber, A. Petraru, M. Fitsilis, R. Meyer, U. Böttger, R. Waser, Microelectr. Eng. 80 (2005) 296.
[4] E.C. Subbarao, J. Phys. Chem. Solids 23 (1962) 665.
[5] K. Morimoto, S. Sawai, K. Hisano, T. Yamamoto, Ferroelectrics 227 (1999) 133.
[6] Y. Shimakawa, Y. Kubo, Y. Nakagawa, T. Kamiyama, H. Asano, F. Izumi, Appl. Phys. Lett. 74 (1999) 1904.
[7] R. Macquart, B.J. Kennedy, B.A. Hunter, C.J. Howard, Y. Shimakawa, Integr. Ferroelectr. 44 (2002) 101.
[8] J.A. Cho, S.E. Park, T.K. Song, M.H. Kim, H.-S. Lee, S.S. Kim, J. Electroceram. 13 (2004) 515.
[9] A.B. Panda, A. Tarafdar, A. Pathak, P. Pramanik, Ceram. Int. 30 (2004) 715.
[10] C. Fujioka, R. Aoyagi, H. Takeda, S. Okamura, T. Shiosaki, J. Eur. Ceram. Soc. 25 (2005) 2723.
[11] B.H. Venkataraman, K.B.R. Varma, J. Phys. Chem. Solids 64 (2003) 2105.
[12] S.M. Zanetti, E.I. Santiago, L.O.S. Bulhões, J.A. Varela, E.R. Leite, E. Longo, Mater. Lett. 57 (2003) 2812.

[13] A. Onodera, K. Yoshio, C.C. Myint, S. Kojima, H. Yamashita, T. Takama, Jpn. J. Appl. Phys. 38 (1999) 5683.
[14] A. Onodera, K. Yoshio, C.C. Myint, M. Tanaka, K. Hironaka, S. Kojima, Ferroelectrics 241 (2000) 159.
[15] K. Yoshio, A. Onodera, H. Yamashita, Ferroelectrics 284 (2003) 65.
[16] J. Yin, Q. He, Y.N. Huang, X.Y. Chen, Z.G. Liu, Phys. Stat. Sol. (a) 168 (1998) 519.
[17] P. Abrman, D. Sedmidubský, A. Strejc, P. Voňka, J. Leitner, Thermochim. Acta 381 (2002) 1.
[18] M. Hampl, A. Strejc, D. Sedmidubský, K. Růžička, J. Hejtmánek, J. Leitner, J. Solid State Chem. 179 (2006) 77.
[19] UniQuant, http://www.uniquant.com/index.html.
[20] W. Schnelle, J. Engelhardt, E. Gmelin, Cryogenics 39 (1999) 271.
[21] J.S. Hwang, K.T. Lin, C. Tien, Rev. Sci. Instrum. 68 (1997) 94.
[22] Quantum Design, Physical Property Measurement System—Application Note, http://www.qdusa.com/pdf/brochures/heat.pdf.
[23] A.T. Dinsdale, Calphad 15 (1991) 317.
[24] J.W. Arblaster, Platinum Met. Rev. 38 (1994) 119.
[25] B. Wilthan, C. Cagran, C. Brunner, G. Pottlacher, Thermochim. Acta 415 (2004) 47.
[26] Inorganic Crystal Structure Database, ver. 1.3.3, FIZ Karlsruhe, NIST Gaithersburg, 2004.
[27] Ismunandar, B.J. Kennedy, Gunawan, Marsongkohadi, J. Solid State Chem. 126 (1996) 135.
[28] Y. Shimakawa, Y. Kubo, Y. Nakagawa, T. Kamiyama, H. Asano, F. Izumi, Appl. Phys. Lett. 74 (1999) 1904.
[29] S.M. Blake, M.J. Falconer, M. McCreedy, P. Lightfoot, J. Mater. Chem. 7 (1999) 1609.
[30] M.A. Zurbuchen, J. Lettieri, S.J. Fulk, Y. Jia, A.H. Carim, D.G. Schlom, S.K. Streiffert, Appl. Phys. Lett. 82 (2003) 4711.
[31] D. Risold, B. Hallstedt, L.J. Gauckler, H.L. Lukas, S.G. Fries, J. Phase Equilib. 16 (1995) 223.
[32] D. Risold, B. Hallstedt, L.J. Gauckler, Calphad 20 (1996) 353.
[33] O. Knacke, O. Kubaschewski, K. Hesselmann, Thermochemical Properties of Inorganic Substances, 2nd ed., Springer, Berlin, 1991.
[34] B. Hallstedt, D. Risold, L.J. Gauckler, J. Am. Ceram. Soc. 80 (1997) 1085.
[35] Y. Akishige, H. Shigematsu, T. Tojo, H. Kawaji, T. Atake, J. Therm. Anal. Calorim. 81 (2005) 537.
[36] Y. Yang, H. Yu, Z. Jin, J. Mater. Sci. Technol. 15 (1999) 203.